ELSEVIER

PII: S0032-3861(97)00176-6

Polymer Vol. 38 No. 25, pp. 6145–6155, 1997

0032-3861/97/$17.00+0.00

Molecular modelling of amorphous membrane polymers

D. Hofmann*, L. Fritz, J. Ulbrich and D. Paul
GKSS Research Center Geesthacht, Institute of Chemistry, Kantstr. 55, D-14513 Teltow, Germany
(Received 13 February 1997)

New results of molecular modelling investigations on the transport of different small molecules in polyimides and polysiloxanes are discussed. The transition state Gusev–Suter Monte Carlo method reveals a reasonable coincidence between simulated and measured diffusivity and solubility values for the polyimides. A comparison between simulation data obtained for flexible chain polymers like poly(dimethyl siloxane) and polyimides shows that the lifetime of temporarily open channels is considerably longer for the stiff chain polymers than for the flexible chain polymers. This is probably a cause for the observed high rate of immediate back-jumps of permeating small molecules during diffusion processes in the polyimides. For amorphous poly(1-(trimethylsilyl)-1-propyne) (PTMSP), equilibrated packing models could be produced with a considerably higher density (1.22 g cm^{-3}) than measured for respective polymer films. This indicates that the low density of the experimentally investigated PTMSP films ($\approx$0.7–0.8 g cm^{-3}) is not the intrinsic 'equilibrium' density but rather caused by the specific membrane preparation conditions. Low density PTMSP, unlike polyimides or polysiloxanes for example, seems to have a microporous morphology. © 1997 Elsevier Science Ltd.

(Keywords: molecular modelling; small molecule diffusion; polyimides)

INTRODUCTION

In two previous papers[1,2] we have reported results of molecular modelling investigations on diffusive and sorptive processes during gas separation and pervaporation processes in flexible and stiff chain dense amorphous polymers. The investigated cases concerned the gas transport (H_2, N_2, O_2) through two polyimides (PI1, PI2)[1] and a poly(amide imide) (PAI)[1] on the one hand and the pervaporation of water/ethanol mixtures through poly(dimethyl siloxane) (PDMS)[2] on the other hand.

It is one aim of this paper to give some new results and additional interpretations of these molecular dynamics (MD) simulations concerning the diffusion processes in the bulk for both types of materials. There also a new material poly(octylmethyl siloxane) (POMS) was considered. Furthermore solubility values in the case of PI1 and PAI have now been calculated utilizing the Gusev–Suter transition state Monte Carlo (MC) method[3–6] in connection with the pcff forcefield[7,8] of Molecular Simulations Inc. (San Diego, CA, USA). The coincidence of these values with the experimental data is much better than in the case of the Widom method with the consistent valence forcefield (cvff)[7,9,10] reported in Hofmann *et al.*[1]. The Gusev–Suter method was also used to calculate diffusivity values from the normal diffusive regime and to obtain a more complete idea about the distribution of free volume in the stiff chain polymer packing models.

A comparison between the simulations of the bulk diffusion in the two types of investigated materials will be utilized to draw a conclusion about a relationship between the possible lifetime of channels between different parts of the free volume (holes) and the rate of immediate back jumps observed in MD.

While glassy polymers usually show considerably lower constants of diffusion for small permeates than rubbery membranes, the respective data for the glassy amorphous poly(1-trimethylsilyl)-1-propyne) (PTMSP) are up to ten times the values obtained for PDMS[11]. This is widely related to the very low density of 0.7–0.8 g cm^{-3} observed experimentally for this material. Therefore, equilibrated PTMSP models were investigated permitting some insight in the molecular packing in this material.

EXPERIMENTAL

Materials and experimental data

Details about the preparation of the PI and PAI membranes and the determination of their permeability and diffusivity parameters can be found elsewhere[1,12]. Literature information about experimental data concerning PTMSP is contained in refs 11, 14–17.

Molecular modelling software and hardware

The models of the molecular packing were constructed and simulated by means of the InsightII/Discover software of Molecular Simulations Inc.[13]. The Molecular Simulations Inc. cvff and pcff forcefield were applied as indicated in the following text. The calculations were performed on IBM RS 6000 workstations and on the CRAY C916 of the DKRZ in Hamburg.

* To whom correspondence should be addressed

Model and simulation details

The repeat units of all investigated materials are shown in *Figure 1*. The construction of equilibrated packing models for the reference polymers PI1 and PAI is described in detail in Hofmann *et al.*[1]. In addition to the MD simulation of the diffusion of N_2 and O_2 molecules in the PI1 mentioned in Hofmann *et al.*[1], using the same simulation conditions, now also a simulation for 10 H_2 molecules in PI1 was performed for 1.2 ns at 300 K. The main aim was to use smaller molecules for the probing of the holes forming the accessible free volume. (*Note*: Experimental data on the diffusion of hydrogen are not available here. Hydrogen is just moving too fast to be measured with the time lag method available for us[12].)

The packing details of the bulk PDMS model, on the other hand, can be found as system II in Fritz *et al.*[2]. Additionally, in the same way, a packing model of POMS was made at the experimental density of 0.91 g cm^{-3} utilizing a 2792 atoms (90 monomers) long chain. This model, including three water and three ethanol molecules, was subsequently subjected to a 1 ns MD run under constant particle number N, constant pressure P, and constant temperature T (NPT) conditions at 300 K.

The PI1 and the PAI (*note*: only the PAI packing number 2 of Hofmann *et al.*[1] was considered here) packing models were subjected to the newly developed transition state theory of Gusev and Suter[3–6]. There first a completely refined amorphous polymer packing cell is made via usual MD techniques. Then the interaction energy of an inserted test gas molecule is calculated on each position of a fine grid layered over the amorphous packing volume element. (*Note*: Usually just the Lennard–Jones and not the Coulomb interaction energy is considered.) Furthermore it is assumed that the polymer packing does not have to undergo structural relaxation (e.g. resulting from torsion transitions) to accommodate an inserted particle. Therefore, this simulation technique is restricted to small molecules (up to methane) which show little electrostatic interaction with the polymer matrix. Using these energy

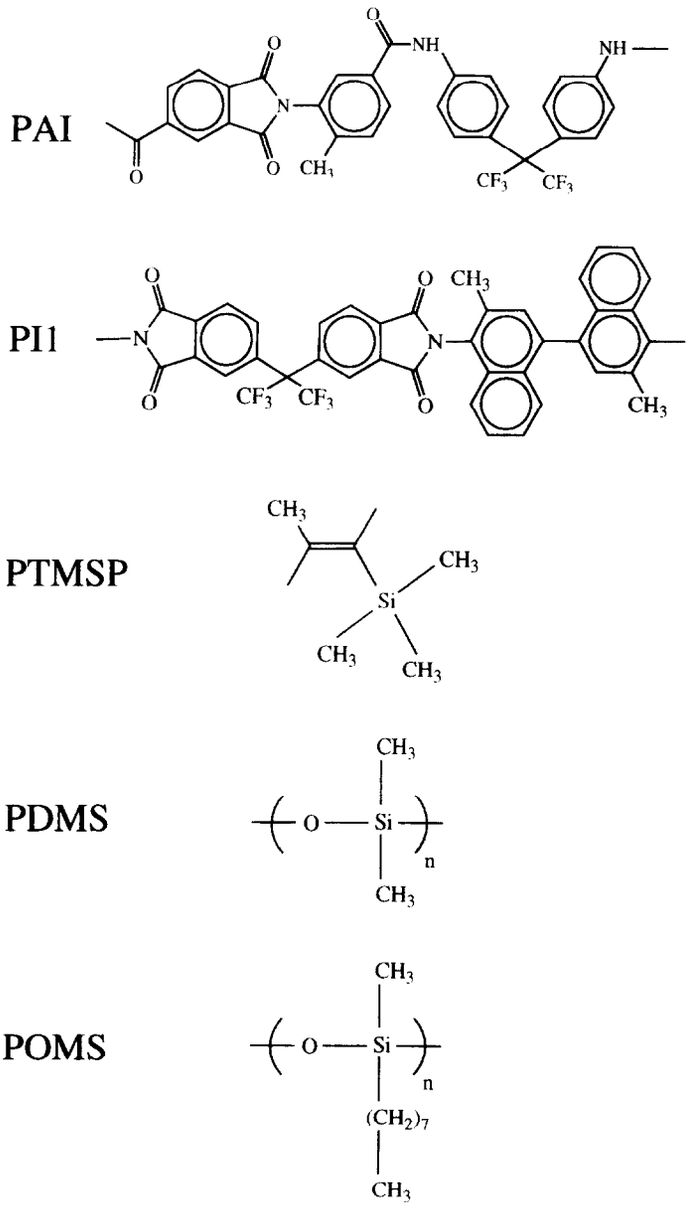

Figure 1 Structure formulae of the repeat units of the investigated polymers

values the whole packing is separated in regions of free volume (low interaction energy) and regions of densely packed polymer (high interaction energy). After this, energetically favourable transition paths between adjacent holes are identified. Each path gets a Boltzmann factor of jump probability assigned. The jump probabilities are influenced by the elastic thermal vibrations of the polymer matrix. This effect is considered via a Debye factor[18]. The main material parameter utilized in this context is $\langle\Delta^2\rangle$, the mean squared displacement (fluctuation) of a polymer atom from its average position. This quantity is usually some fraction of an Ångström and can be either estimated or obtained from a short MD run for the polymer without penetrant molecules. Having determined appropriate jump probabilities, the diffusion of gas particles can then be simulated via a MC type procedure. The main advantage of this method is that much less computer time is consumed permitting much longer simulation times than MD. There is, however, a loss of atomistic detail as compared with MD.

The pcff forcefield was utilized for all of these calculations. There the van der Waals interactions between the atoms of a polymer packing and an inserted penetrant molecule are described by a 9–6 potential where r_{ij} is the distance (in Ångström) between a given polymer atom j from the penetrant i:

$$\sum_j \varepsilon_{ij}\left[2\left(\frac{\sigma_{ij}}{r_{ij}}\right)^9 - 3\left(\frac{\sigma_{ij}}{r_{ij}}\right)^6\right]$$

with

$$\sigma_{ij} = \left[\frac{\sigma_i^6 + \sigma_j^6}{2}\right]^{1/6} \quad \text{and} \quad \varepsilon_{ij} = 2\sqrt{\varepsilon_i \varepsilon_j}\,\frac{\sigma_i^3 \sigma_j^3}{\sigma_i^6 + \sigma_j^6} \qquad (1)$$

To use this term, united atom representations[6] of the forcefield parameters σ_i and ε_i were chosen for the respective penetrant H_2, N_2 and O_2 molecules:

$H_2: \sigma_i = 2.928$ Å and $\varepsilon_i = 0.0735$ kcal mol^{-1}
$N_2: \sigma_i = 3.698$ Å and $\varepsilon_i = 0.1889$ kcal mol^{-1}
$O_2: \sigma_i = 3.460$ Å and $\varepsilon_i = 0.2344$ kcal mol^{-1}

The spacing of the cubic lattice for the insertion of the probe molecules was 0.03 nm. The smearing factor was determined via a so-called self-consistent field procedure[5] employing the mean squared displacement $s(t)$ of the respective polymer atoms. $s(t)$ was obtained from 10–20 ps MD runs with snapshots taken every 100 fs. The trajectory of each penetrant molecule was simulated for 10^{-4}–10^{-3} s. The resulting mean squared displacement curves were obtained as averages over at least 1000 penetrants in each case.

PTMSP was included in the investigation because of its already mentioned extraordinary permeability properties. The utilized packing model shall now be characterized in more detail: an atactic model chain with a 50/50 probability for the occurrence of monomers with *cis* and *trans* configuration was constructed from 200 monomers (3802 atoms). Just head-to-tail connections between adjacent monomers were considered as suggested by the literature[14]. The initial packing density was 0.75 g cm^{-3} resulting in a packing cell side length of 3.68 nm. A modified Theodorou–Suter[19,20] approach provided by the Amorphous-Cell module of the InsightII/Discover software utilizing the pcff forcefield[7,13] was used for the chain packing. The model polymer packing was then refined utilizing the multistage techniques described in refs 1 and 2. Sequences of static structure optimizations and MD simulations combined with forcefield parameter scaling were utilized for this purpose. The following conditions were used:

(i) Minimum image periodic boundary conditions to make the systems numerically tractable and to avoid artificial symmetry effects.
(ii) Cut-off distance for all nonbond interactions 1.5 nm with a smooth switching function being used for all interatomic distances between 1.1 and 1.3 nm. At 1.3 nm the nonbond interactions between two atoms are considered to be exactly zero. The distance interval between 1.3 and 1.5 nm is necessary as a buffer because the list of atom-pairs for which the nonbond interaction energy needs to be calculated is updated only about every 20 time steps. This considerably speeds up the simulations. The buffer width then accounts for the fact that during 20 time steps some additional pairs of atoms might decrease their distances below 1.3 nm.
(iii) Simulation time step 1 fs.
(iv) Berendsen method[21] of temperature and pressure bath coupling with a coupling constant of 100 fs to stabilize the intended system temperature and pressure during MD runs.

Evaluation of data

The coefficient of diffusion D for a simulated small penetrant molecule in a polymer matrix can be calculated from the mean squared displacement $s(t) = \langle|\mathbf{r}(t) - \mathbf{r}(0)|^2\rangle$ of this molecule averaged over all possible time origins $t = 0$ via the Einstein equation:

$$D = \langle|\mathbf{r}(t) - \mathbf{r}(0)|^2\rangle/6t \qquad (2)$$

Here, $\mathbf{r}(t)$ is the Cartesian position vector of a permeant molecule at time t.

In Hofmann *et al.*[1] the Widom particle insertion method[22] was used to estimate the solubility S of a given gas in a polymer. S gives the concentration c of gas in a volume element of the polymer that is in equilibrium with an outside pressure reservoir of this gas. As far as the determination of solubility values is concerned the Gusev–Suter and Widom methods are completely equivalent. The only methodical difference is that in the Widom method virtual gas particles are inserted at random positions in a completely refined model polymer matrix while in the Gusev–Suter case the insertion is performed on all grid points of a regular cubic lattice layered onto the packing model. In both cases the insertion procedure is followed by a calculation of the interaction energy E of an inserted particle with the polymer. Then the excess thermodynamic potential μ_{ex} is obtained via

$$\mu_{ex} = RT\ \ln\langle\exp\,(-E/kT)\rangle \qquad (3)$$

S in turn is related to μ_{ex} over the relation

$$S = \exp(-\mu_{ex}/RT) \qquad (4)$$

with k and R being the Boltzmann constant and the gas constant, respectively. The 'experimental' solubility data S_{exp} were estimated from the ratio of measured permeabilities P_{exp} and diffusivities D_{exp}

$$S_{exp} = P_{exp}/D_{exp} \qquad (5)$$

RESULTS AND DISCUSSION

As a first step of MD data evaluation, the movement of the simulated permeant molecules through the polymer is usually characterized qualitatively and quantitatively[1,2,23–35]. These investigations generally showed that the diffusion of small gas molecules through amorphous polymers consists of two different modes of motion. Over relatively long periods of time (typically a few 100 ps) the gas molecules just explore distinct holes in the polymer. Thereby they are reflected by the polymer matrix about every 1–2 ps. In this mode of motion the permeant molecules act as probes for the shape of the visited free volume.

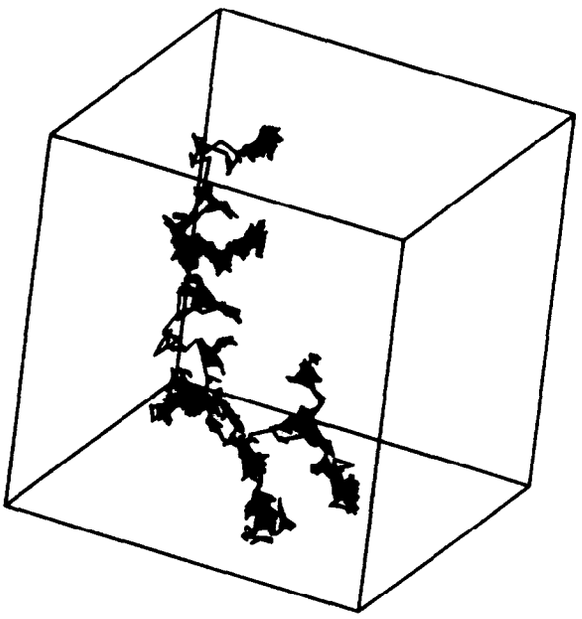

Figure 2 Path of a hydrogen molecule through the polyimide matrix PI1. (Note, that here, due to the very fast movement of the penetrants, the length of the shown box is 12.8 nm, i.e. four times the packing cell length)

Figure 2 reveals the path of a hydrogen molecule through the PI1 matrix. This trajectory was taken over 1 ns. The figure shows that the free volume of this polymer consists of many small cavities. *Figure 2* also leads to the second mode of motion, a hopping mechanism. Sometimes channels between adjacent holes are opening up for a short time, which under favourable circumstances (permeant molecule flying with the right momentum) permit permeating molecules to jump from one hole to the next. It is obvious that the diffusive movement of permeant molecules through an amorphous polymer is only determined by these jumps.

Utilizing the obtained MD data it is possible to have an even closer look at the structural changes in a polymer that permit the formation of channels between adjacent portions (holes) of the free volume. As an example *Figure 3* shows a sequence of 0.35 nm thick slices cut out of the POMS packing along the c-axis during a jump event for a water molecule occurring between $t = 429$ ps and $t = 444$ ps. It should be noticed that all slices were taken from the same c-axis range around the mentioned jump. Some aspects are remarkable:

(1) The cross section of the holes is not always much larger than the penetrant molecule.
(2) The temporary channels can be quite broad up to a transient coalescence of two holes (cf. *Figure 3* at $t = 436.5$ ps).
(3) The backbone atoms remain almost fixed over the whole jump event.
(4) However, relatively large scale segmental motions mainly of the octyl side chains are necessary to open/close a channel. This can be related to the fact that the packing of POMS segments is relatively dense (cf. *Figure 3*). In Fritz *et al.*[2] a similar representation of a jump event in PDMS was shown (cf. *Figure 3* in Fritz *et al.*[2]). There a less pronounced movement of the polymer atoms in the vicinity of a jump event could be found. This behaviour seems to be due to the less dense chain packing (higher amount of free volume) which makes

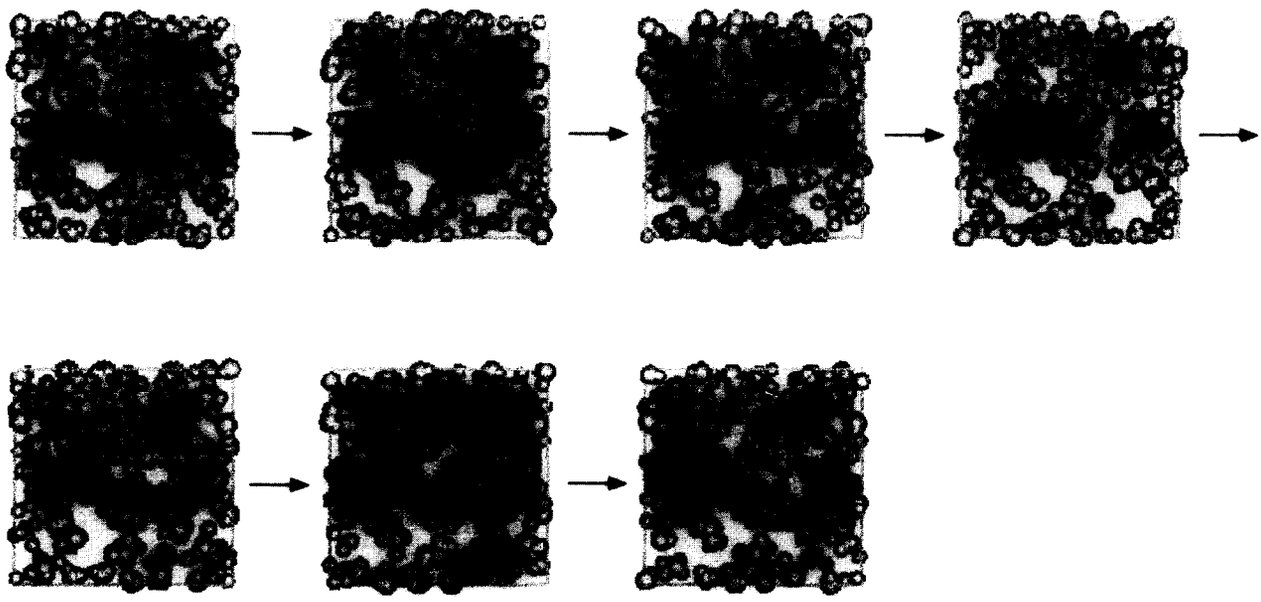

Figure 3 Series of 0.35 nm thick slices through the POMS packing model showing the jump event of a water molecule occurring between $t = 429$ ps and $t = 444$ ps. The slices were taken every 1.5 ps. The colors are: light grey for side chain atoms, black for the jumping water molecule and dark grey for the backbone atoms

Table 1 Comparison between measured D_{exp} and calculated D_{calc} average diffusion coefficients for the investigated polymers. The calculated values were obtained from detailed atomistic MD simulations. For PDMS also some literature results are shown for comparison

Polymer	Ref.	Penetrant	$\langle D_{calc} \rangle$ (10^{-7} cm^2 s^{-1})	$\langle D_{exp} \rangle$ (10^{-7} cm^2 s^{-1})
	2	H_2O	130	145
	2	ethanol	44	45
PDMS	33, 34	H_2O	153	145
	33, 34	ethanol	20	45
	26	CH_4	210	206
	2	H_2O	31	n.a.
POMS	2	ethanol	7	n.a.
	11	CH_4	n.a.	65
PAI	1	H_2	47	9.4
PI1	1	O_2	32	7.4
		N_2	12	2.8
	This paper	H_2	355	n.a.

jumps in this material easier than in, for example, POMS. The finding that in the case of the more densely packed POMS (connected with a higher glass transition temperature than in PDMS) larger motions of the polymer segments are necessary to allow for a penetrant jump than in PDMS, is certainly a main reason for the fact that the constants of diffusion for POMS are considerably lower than for PDMS (cf. *Table 1*).

It should be mentioned that the observation of large scale segmental motions in the region of permeant jumps in POMS is in line with recent suggestions made by Koros[36] which were derived from a more experimental point of view concerning other densely packed polymers.

The average extent to which a permeant molecule moves away from its origin over a certain amount of time determines how fast the diffusion of a given permeant

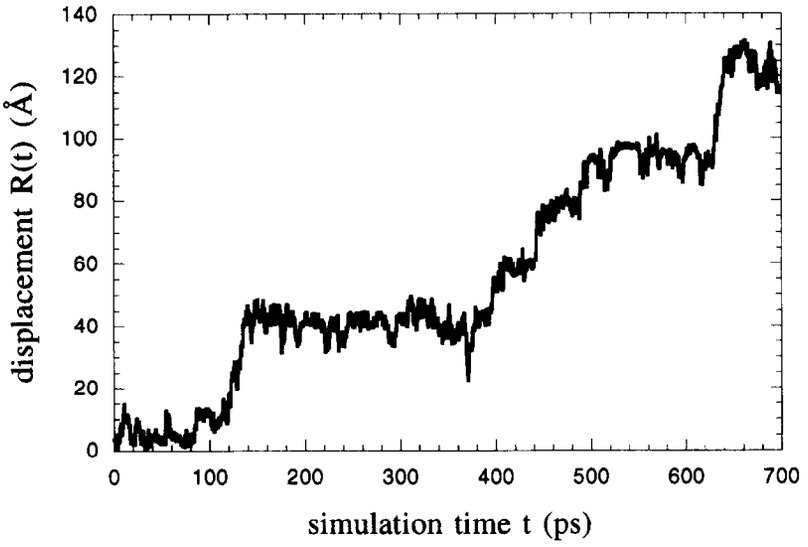

Figure 4 Displacement $R(t)$ of the hydrogen molecule shown in *Figure 3* (t = simulation time)

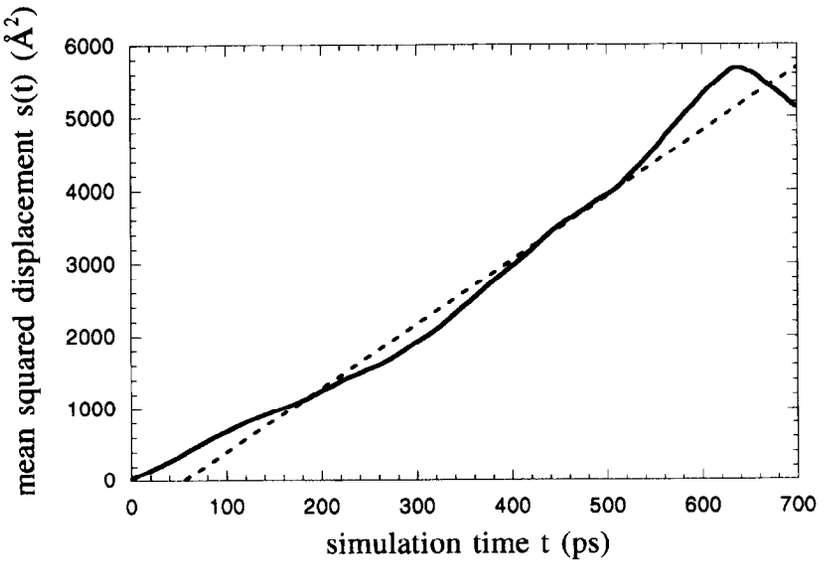

Figure 5 Mean squared displacement $s(t)$ of the hydrogen molecule shown in *Figure 3*

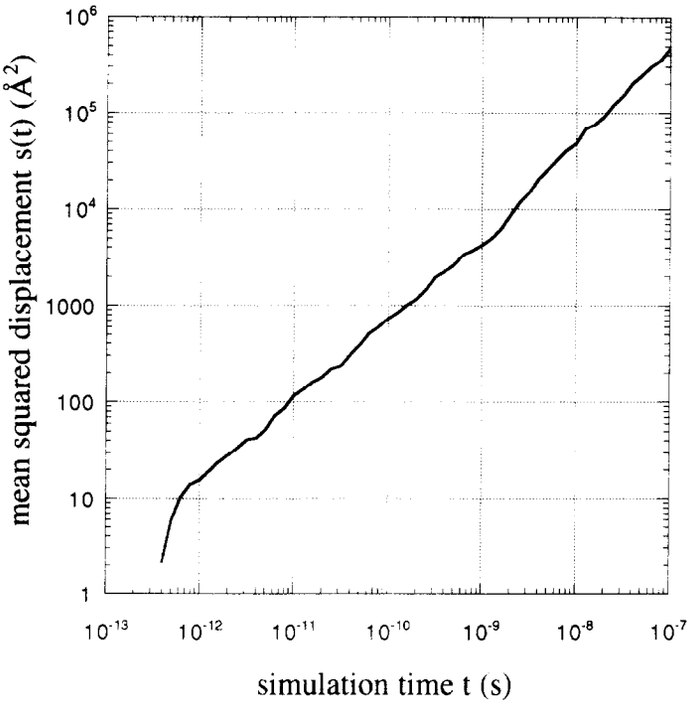

Figure 6 Log[$s(t)$] vs. log(t) plot obtained from the Gusev–Suter transition state Monte-Carlo procedure for a hydrogen molecule in the poly(amide imide) PAI mentioned in *Table 1*

Table 2 Comparison between diffusivities and solubilities obtained from the Gusev–Suter method, D_{Gusev} and S_{Gusev}, and experimental data, D_{exp} and S_{exp}, for PAI and PI1

Polymer	Penetrant	D_{Gusev} (10^{-7} cm^2 s^{-1})	D_{exp} (10^{-7} cm^2 s^{-1})	S_{Gusev} (bar^{-1})	S_{exp} (bar^{-1})
PAI	H_2	15.9	9.4	0.09	0.11
PAI	O_2	0.4	0.3	1.24	0.40
PAI	N_2	0.2	0.1	0.54	0.29
PI1	O_2	15.3	7.4	5.50	2.16
PI1	N_2	2.6	2.8	3.77	1.65

species is. *Figure 4* shows the displacement $R(t) = \sqrt{[\mathbf{r}(t) - \mathbf{r}(0)]^2}$ of the hydrogen molecule already discussed in *Figure 2*. One can clearly identify the very fast oscillations inside one and the same hole and distinct jumps between different holes.

From the data shown in *Figure 4* the mean squared displacement $s(t) = \langle|\mathbf{r}(t) - \mathbf{r}(0)|^2\rangle$ of a molecule averaged over all possible time origins may be calculated. *Figure 5* shows a $s(t)$ vs. t plot again for the hydrogen molecule mentioned.

These plots are often averages over all simulated permeant molecules and do usually contain a more or less extended linear portion and a noisy part at longer times[23–35]. The nonlinear portion of the curve is caused by statistical problems. From the linear part, the constant of diffusion D may be evaluated using equation (2).

Usually the constant of diffusion obtained from a MD simulation should be basically the same as the measured constant of diffusion of a real transport process. Thus, the coincidence between calculated and measured D values, D_{calc} and D_{exp}, respectively, may serve as a quality criterion for the performed MD simulation. Some sources of possible systematic errors need to be mentioned. The so-called anomalous diffusion that was first reported by Müller-Plathe *et al.*[23,27] constitutes one of the problems for the calculation of D values from MD simulations. The Einstein equation [equation (2)] relies on the assumption of a random walk for each simulated particle through the polymer matrix. That means that the jumps of the gas molecules between individual holes in the free volume must determine the $s(t)$ behaviour. The still rather short possible duration of MD simulations (up to 10 ns) does, however, result in a non-negligible influence of the very fast movement of permeate molecules (timescale several hundred picoseconds) inside the individual holes on $s(t)$. This in-hole motion is determined by the shape of the holes and is therefore no random walk. The usual effect of anomalous diffusion is to create a somewhat smaller slope of the $s(t)$ curve at lower t values. (More exact: the Einstein equation holds true if the slope of a plot of the logarithm of the mean squared displacement as a function of the logarithm of the simulation time, $\log[s(t)] = f[\log(t)]$, is equal to one. The influence of this problem may extend up to several nanoseconds.)

Another obstacle for accurate predictions of D values consists of the fact that in a real amorphous polymer each volume element shows a different packing of chain segments, while MD simulations can be performed only for at maximum a few packing cells.

The problems mentioned so far indicate that it would need much longer MD simulation times and much

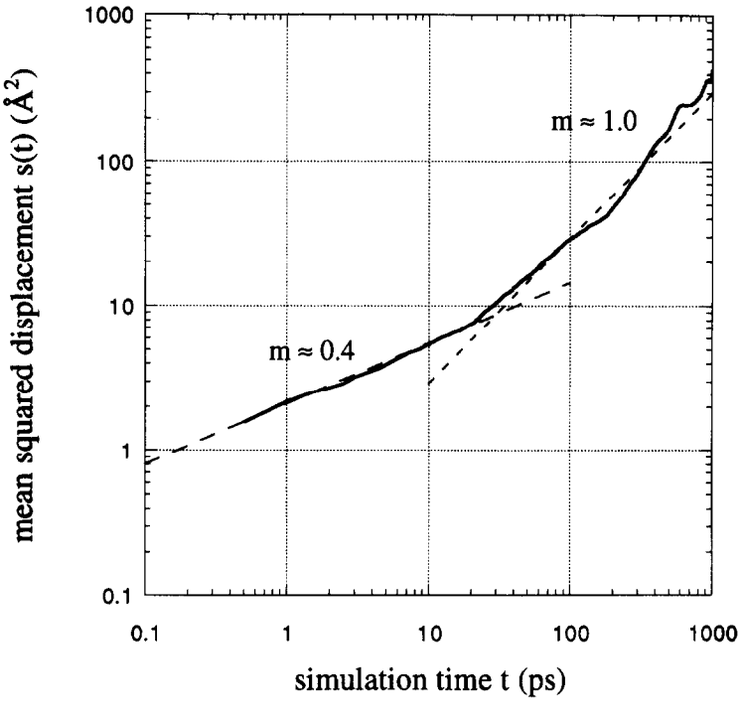

Figure 7 Log[$s(t)$] vs. log (t) plot for the diffusion of a water molecule in POMS obtained from a completely atomistic MD run (solid line) with m = slope

more different packing cells for each polymer–permeate system to obtain D values very close to reality. This is out of scope of the presently available hardware power. It is, however, nevertheless usually possible to predict the right order of magnitude of D for relatively fast diffusion processes ($D > 10^{-7}\,cm^2\,s^{-1}$). This is demonstrated in *Table 1* which contains average simulated and measured data for the investigated PAI, PI1, PDMS and POMS polymers.

However, the already mentioned newly developed transition state theory of Gusev and Suter[3–5] can be helpful for more exact predictions of the diffusion coefficient. *Figure 6* shows a log[$s(t)$] vs. log (t) plot obtained with the Gusev–Suter method for a hydrogen molecule in the PAI which was already quoted in *Table 1*. A slope $m < 1$ can be recognized for $t < 2$ ns. Up to this time anomalous diffusion is dominating while for $t > 2$ ns real Einstein diffusion with $m \approx 1$ is observed. It can be stated that in this case the deviation between anomalous and normal diffusion behaviour as indicated by the slope m is not very considerable. As already mentioned, the determined average interaction energy between a test molecule and the polymer packing can also be employed for the calculation of the solubility for the test permeant[3–5]. *Table 2* illustrates the potential predictive capabilities of this new simulation technique for PI1 and a PAI packing (cf. PAI packing no. 2 in Hofmann *et al.*[1]). [*Note*: In the cases of PDMS and POMS the normal diffusion regime was reached during the time (1 ns) of the MD simulation (cf. *Figure 7*).]

The good agreement between experimental and calculated data is a proof that the employed packing models are of acceptable quality. Here, particularly, the solubility is important as was pointed out by van der Vegt *et al.*[37].

In Hofmann *et al.*[1] the Widom[22] method in connection with the cvff forcefield was used to determine solubility values for PAI and PI1. The calculated S_{calc} data were up to three orders of magnitude higher than the experimental ones S_{exp}. As can be seen from *Table 2*, the coincidence between measured and experimental data is much better in the case of the Gusev–Suter method used with pcff. In principle, the Gusev–Suter method should produce the same solubility values as the Widom technique. Therefore, the pcff forcefield seems to be much better suited for this kind of calculation. The problem with cvff seems to consist in the applied specific implicit consideration of hydrogen bonds via manipulated Lennard–Jones and electrostatic terms. Since the utilized solubility calculations do not consider electrostatic terms, severe systematic errors may arise for polymers containing atoms which may form hydrogen bonds if just manipulated Lennard–Jones and not the compensating electrostatic terms are employed.

It is certainly useful to have a closer look at the free volume of the simulated polymer models. The most simple way is to consider the small permeating molecules as probes for the free volume as can be seen from *Figure 3*. Of course, in this way the free volume visited by the simulated particles can be visualized. A more systematic free volume probing also exists on the basis of the Gusev–Suter transition state theory as described above[3–5,32]. There the calculated change of the system energy ΔE (with and without the inserted particle) at any lattice point is utilized in the following way. Negative (binding) or small positive (probe molecule in the vicinity of a polymer atom) ΔE indicate that a lattice point belongs to the free volume of the sample. A considerably positive (repulsive) ΔE on the other hand reveals that the probe molecule has hit a polymer atom. *Figure 8* shows a free volume map obtained in this way for the PI1 model system. (*Note*: In this case an oxygen molecule was used as a probe molecule.) It should be mentioned that there exists a certain ambiguity from which interaction energy on a lattice point is considered to form a part of the free volume. To partly resolve this

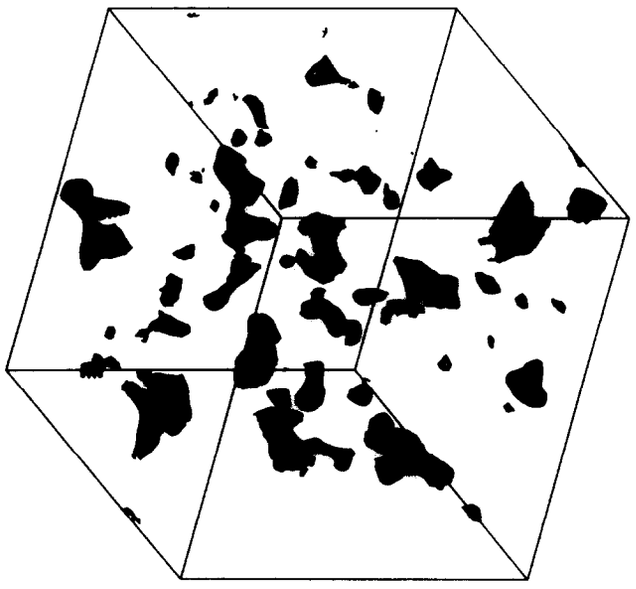

Figure 8 Free volume map obtained for the packing model of the polyimide utilizing the Gusev–Suter method

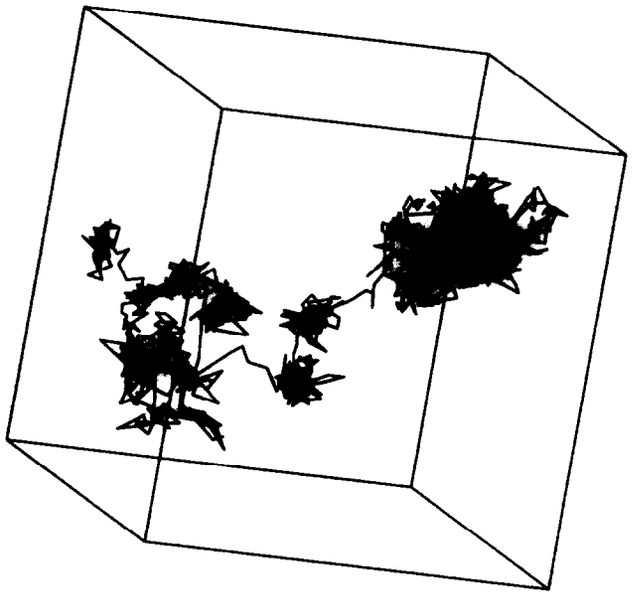

Figure 9 Trajectory of a water molecule in PDMS

problem simpler pictures like *Figure 2* may be used as a standard for the expected average void size in a polymer.

Figure 9 contains the trajectory of a water molecule in PDMS (cf. Fritz *et al.*[2]). It shows the typical relatively homogeneous free volume distribution in flexible chain polymers. The individual voids forming the free volume are clearly separated from each other. The detailed evaluation of the particle movement did not show any immediate back jumps (2) → (1) after a jump from one hole (1) to another (2). In the stiff chain polymers (PI1 and PAI)[1] on the other hand, the individual holes were closer to each other (cf. *Figure 2*) and a rather large number of immediate back jumps occurred. This indicates that once a channel between two adjacent holes in a stiff chain polymer is formed it will stay open for at least some 100 ps, making the mentioned back jumps much more probable than a jump to any other adjacent hole. This special channel behaviour seems to be one cause for the general tendency that the constants of diffusion for small molecules are smaller in stiff chain polymers than in flexible chain rubbery polymers.

There is one prominent exception from this rule, the glassy stiff chain poly(1-(trimethylsily)-1-propyne) (PTMSP) showing about the same constants of diffusion and up to ten times the permeabilities of the rubbery PDMS[11,14–17]. This behaviour is widely related with the exceptionally low density observed for this material which might even lead to permanent diffusion channels[38]. The reported specific density values vary between 0.70 and 0.77 $g\,cm^{-3}$ with a certain aging tendency towards higher values.

To have a closer look at the structural causes for the specific behaviour of PTMSP the relaxed packing model obtained as described above for a density of 0.75 $g\,cm^{-3}$, was subjected to a 1 bar constant pressure NPT-MD run to check whether the refined system met the density criterion at normal pressure conditions. There the PTMSP showed an unexpected behaviour. In the case of 1 bar simulations of stiff chain glassy polymers it is usually very laborious to achieve a chain packing showing a high density as measured. Often the volume of the model structure is just increasing due to unrealistic tensions. For the PTMSP equilibrated under constant volume conditions at a density of 0.75 $g\,cm^{-3}$ on the other hand the 1 bar MD run very quickly (after 10 ps) led to a density increase to about 0.85 $g\,cm^{-3}$. This behaviour indicated that the PTMSP obtained under the polymerization and film formation conditions reported so far in the literature is not in the most dense ('equilibrium') packing state possible. That means the PTMSP materials obtained by now might be microporous. (*Note*: This hypothesis is also supported by the fact that the measured density values are very far below the values reported for any other glassy stiff chain polymer). To get an idea about the possible density of a hypothetical really dense PTMSP the following MD procedure was applied which partly resembles the one employed in Hofmann *et al.*[1] to predict the density of a hypothetical polyimide polymer (PI2):

(1) a constant pressure MD run at 8000 bar, 303 K for about 10 ps. This procedure brought the system density to 1.06 $g\,cm^{-3}$.
(2) a refinement procedure consisting of a sequence of static structure optimizations and MD simulations combined with forcefield parameter scaling.

A subsequent 1 bar/303 K MD simulation resulted in a further density increase to a stable value of 1.22 $g\,cm^{-3}$. At the same time the length of the packing model decreased to 3.12 nm. *Figure 10* contains a series of 0.5 nm thick slices cut through an equilibrated high density PTMSP packing model revealing the typical behaviour found also for other dense stiff chain glassy polymers of comparable or higher density. (*Note*: While *Figure 3* contains a time sequence of slices at always one and the same position, *Figure 10* such as *Figure 11* show almost the whole packing cell slice by slice at one and the same simulation time.)

A few remarks are necessary concerning the interpretation of the simulated high density PTMSP structure:

(1) There are no published data about geometric isomerism in PTMSP. We have, therefore, chosen the most irregular case (atactic sequence of 50% *cis*

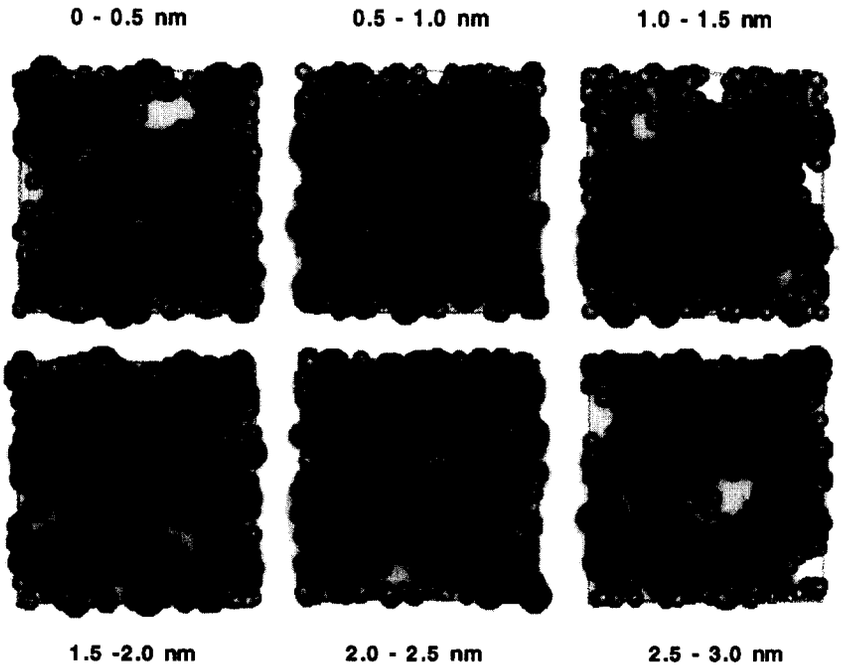

Figure 10 Series of 5 nm thick slices along the *c*-axis of an equilibrated PTMSP packing model of a density of 1.22 g cm^{-3}. Each slice is identified by its minimum and maximum *c*-coordinates

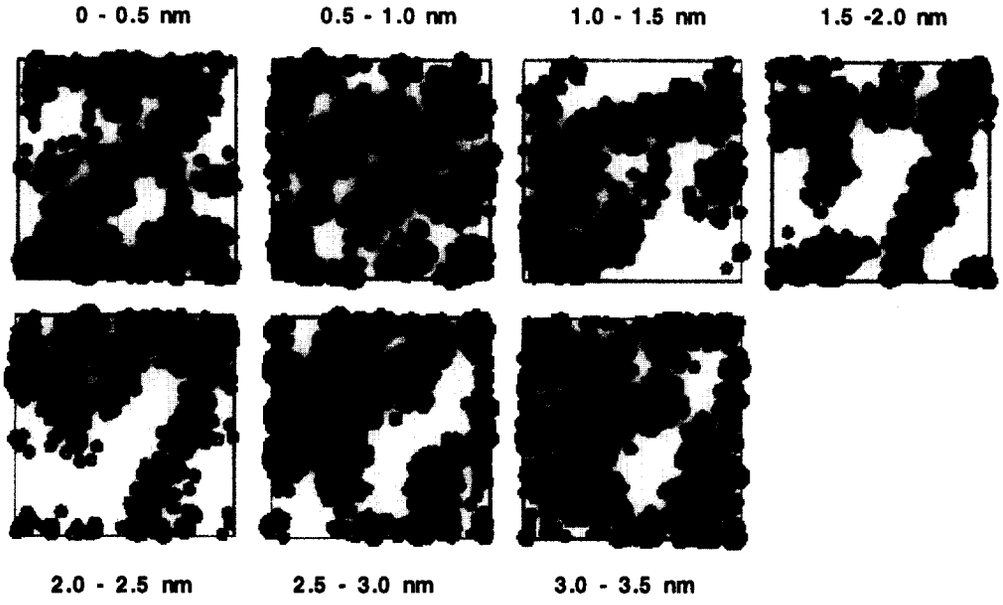

Figure 11 Series of 5 nm thick slices along the *c*-axis of an equilibrated PTMSP packing model of a density of 0.75 g cm^{-3}. Each slice is identified by its minimum and maximum *c*-coordinates

and 50% *trans* isomers) for the simulated model packing. Thus, the simulated density might somewhat change if appropriate experimental information about the polymer structure would become available.

(2) Doghieri *et al.*[39,40] have developed a new Non Equilibrium Lattice Fluid (NELF) model for the description of the thermodynamic properties of polymer penetrant mixtures in the glassy state. In the case of PTMSP, which was considered to be composed of dense polymer regions and extended holes, a polymer partial density parameter of 1.25 g cm^{-3} was given, i.e. a value very close to the simulated 'equilibrium' density necessary for a good fit of this theory to experimental data.

(3) As already stated above the low density real PTMSP materials may be considered to be microporous but basically homogeneous. Volkov[41], however, suggested that this material showed a considerably inhomogeneous structure made of relatively large interconnected holes (with a narrowest diameter of 0.4 nm) side by side with rather densely packed polymer regions extending over several nm. If this assumption could be proven, the density of dense PTMSP simulated by us could also possibly be assigned to the densely packed polymer domains in

the Volkov model for the low density experimentally obtained PTMSP.

To check whether MD simulations can give an idea about the molecular packing status in low density PTMSP *Figure 11* was prepared. It contains a series of 0.5 nm thick slices cut through an equilibrated PTMSP packing model of density 0.75 g cm^{-3}. (*Note*: Similar figures prepared from other equilibrated low density PTMSP packing models revealed a comparable behaviour.) The picture indicates a considerable degree of heterogeneity. The holes extend up to about 2 nm and are widely interconnected. In addition regions of relatively densely packed polymer chain segments can be observed. It must be clearly stressed, however, that considering the size of the observed holes the applied model size of about 3.7 nm side length is probably still considerably too small to derive any quantitative results. On the other hand, it seems to be possible to interpret these simulation data as showing the right qualitative tendency of the molecular packing status in low density PTMSP. Thus, these results would support the ideas of, for example, Volkov[41] and Singh *et al.*[38] about the free volume topology in this material. The large amount of empty space in the low density PTMSP does confirm our suggestion that it should also be possible to prepare this polymer with a much higher density (above 1.2 g cm^{-3}).

SUMMARY

For rubbery polymers like PDMS or POMS discussed in this paper, often completely atomistic MD simulations of about 1–2 ns can be sufficient for the calculation of diffusion coefficients in the normal regime for small molecules. In the case of stiff chain glassy polymers like PAI and PI1, however, the use of the Gusev–Suter MC techniques was utilized to extend the diffusion simulation beyond the anomalous region. In this way the coincidence between calculated and simulated diffusivities could be considerably improved (cf. *Tables 1* and *2*). It was also possible to obtain solubilities very close to measured data. But even this rather fast simulation technique will not lead to a fast predictability of membrane transport parameters for large numbers of hypothetical amorphous polymers in the near future. This is mainly due to the fact, that the construction of well equilibrated amorphous polymer packing models is still demanding large amounts of computer time.

Perhaps even more important than the possible prediction of quantitative membrane parameters is that the evaluation of completely atomistic MD simulations permits a deeper insight into the mechanism underlying an investigated transport process. One example discussed was the possibility to visualize the distribution of free volume (cf. *Figures 2, 3, 8–11*) and its dynamic behaviour, e.g. during individual penetrant jumps (cf. *Figure 3* in this paper and Figure 3 in Fritz *et al.*[2]).

Another finding was that there seems to be at least one important difference between small particle diffusion in the stiff chain polyimides and flexible polymers like the investigated polysiloxanes. It consists of stiff chain polymers in a considerably higher rate of immediate back jumps of penetrant molecules from a just-reached hole to the hole they started from. Obviously, for the polyimides, the temporary channels between adjacent parts of the free volume are open for longer times than in the case of flexible chain packings. This in turn may be one reason for the usually lower constants of diffusion in stiff chain polymers.

The MD investigation of PTMSP suggests that the very low experimental density values obtained so far for this material are probably far below the maximum possible ('equilibrium') density. Or, in other words, choosing a different way of preparing PTMSP films may lead to samples with much higher densities which then would show much lower permeabilities. The experimentally obtainable PTMSP seems to reveal a microporous morphology making it qualitatively different from the polyimides and polysiloxanes also investigated.

ACKNOWLEDGEMENTS

The authors are greatly indebted to Dr D. Fritsch, Dr K.-V. Peinemann (GKSS in Geesthacht, Germany) and Dr Müller-Plathe (MPI of Polymer Science in Mainz, Germany) for valuable discussions. Furthermore, the support of the Fonds der Chemischen Industrie (Germany) is gratefully acknowledged.

REFERENCES

1. Hofmann, D., Ulbrich, J., Fritsch, D. and Paul, D., *Polymer*, 1996, **37**, 4773.
2. Fritz, L. and Hofmann, D., *Polymer*, 1997, **38**, 1035.
3. Gusev, A. A., Arizzi, S. and Suter, U. W., *J. Chem. Phys.*, 1993, **99**, 2221.
4. Gusev, A. A. and Suter, U. W., *J. Chem. Phys.*, 1993, **99**, 2228.
5. Gusev, A. A. and Suter, U. W., *Computer-aided Mat. Design*, 1993, **1**, 63.
6. The Gusev–Suter computations were performed using the gsnet and gsdif programs developed by A. Tiller of Molecular Simulations Inc.
7. Discover User Guide, version 2.3.5. San Diego: Biosym Technologies, 1994.
8. Sun, H., Mumby, S. J., Maple, J. R. and Hagler, A. T., *J. Am. Chem. Soc.*, 1994, **116**, 2978.
9. Hagler, A., Lifson, S. and Dauber, P., *J. Am. Chem. Soc.*, 1979, **101**, 5122.
10. Hagler, A., Lifson, S. and Dauber, P., *J. Am. Chem. Soc.*, 1979, **101**, 5131.
11. Stern, S. A., *J. Membrane Sci.*, 1994, **94**, 1.
12. Fritsch, D. and Peinemann, K.-V., *J. Membrane Sci.*, 1995, **99**, 29.
13. Computational results obtained from software programs from Molecular Simulations Inc. of San Diego—Static and dynamic calculations were done with the Discover® program, using the cvff and pcff forcefields. The amorphous packings were obtained with the help of the Amorphous Cell module. Some data evaluations were performed and graphically displayed utilizing the InsightII® molecular modeling system.
14. Masuda, T., Isobe, E. and Higashimura, T., *Macromolecules*, 1985, **18**, 841.
15. Takada, K., Matsuya, H., Masuda, T. and Higashimura, T., *J. Appl. Polym. Sci.*, 1985, **30**, 1605.
16. Icharaku, Y. and Stern, S. A., *J. Membrane Sci.*, 1987, **34**, 5.
17. Plate, N. A., Bokarev, A. K., Kaliuzhnyi, N. E., Litvinova, E. G., Khotimskii, V. S., Volkov, V. V. and Yampol'skii, Yu. P., *J. Membrane Sci.*, 1991, **60**, 13.
18. Debye, P., *Verh. Deut. Physik. Ges.*, 1913, **15**, 783.
19. Theodorou, D. N. and Suter, U. W., *Macromolecules*, 1985, **18**, 1467.
20. Theodorou, D. N. and Suter, U. W., *Macromolecules*, 1986, **19**, 139.
21. Berendsen, H. J. C., Postma, J. P. M., van Gunsteren, W. F., DiNola, A. and Haak, J. R., *J. Chem. Phys.*, 1984, **81**, 3684.
22. Widom, B., *J. Chem. Phys.*, 1963, **39**, 2808.
23. Müller-Plathe, F., *Acta Polymer*, 1994, **45**, 259.

24. Gusev, A. A., Müller-Plathe, F., van Gunsteren, F. W. and Suter, U. W., *Advances in Polymer Science*, 1994, **16**, 207.
25. Sok, R. M. and Berendsen, H. J. B., *Polym. Prepr.*, 1992, **33**, 641.
26. Sok, R. M., Berendsen, H. J. C. and van Gunsteren, W. F., *J. Chem. Phys.*, 1992, **96**, 4699.
27. Müller-Plathe, F., Rogers, S. C. and van Gunsteren, W. F., *Chem. Phys. Lett.*, 1992, **199**, 237.
28. Müller-Plathe, F., *J. Chem. Phys.*, 1991, **94**, 3192.
29. Müller-Plathe, F., *J. Chem. Phys.*, 1992, **96**, 3200.
30. Smit, E., Mulder, M. H. V., Smolders, C. A., Karrenbeld, H., van Eerden, J. and Feil, D., *J. Membrane Sci.*, 1992, **73**, 247.
31. Gunsteren, W. F. van and Berendsen, H. J. C., *Angewandte Chemie*, 1990, **29**, 992.
32. *Polymer User Guide*, Amorphous Cell Section, version 6.0 San Diego: Biosym Technologies, 1993.
33. Tamai, Y., Tanaka, H. and Nakanishi, K., *Macromolecules*, 1995, **28**, 2544.
34. Tamai, Y., Tanaka, H. and Nakanishi, K., *Fluid Phase Equilibria*, 1995, **104**, 363.
35. Müller-Plathe, F., Rogers, S. C. and Gunsteren, W. F. van, *Macromolecules*, 1992, **25**, 6722.
36. Koros, W. I., *Proceedings of the ICOM'96 International Congress on Membranes and Mebrane Processes*, Yokohama, 1996, p. 36.
37. Vegt, N. F. A. van der, Briels, W. J., Wessling, M. and Strathmann, H., *J. Chem. Phys.*, 1996, **105**, 8849.
38. Singh, A., Morisato, A., Freeman, B. D., Casillas, C. and Pinnau, I., *Proceedings of the ICOM'96 International Congress on Membranes and Membrane Processes*, Yokohama, 1996, p. 277.
39. Doghieri, F., Biavati, D. and Sarti, G. C., *Proceedings of the ICOM'96 International Congress on Membranes and Membrane Processes*, Yokohama, 1996, p. 282.
40. Doghieri, F. and Sarti, G. C., *Macromolecules*, 1996, **29**, 7885.
41. Volkov, V. V., *Proceedings of the ICOM'96 International Congress on Membranes and Membrane Processes*, Yokohama, 1996, p. 280.